EXPERIMENTAL BENCHMARK WING-BOX WITH ADJUSTABLE STIFFNESS AND CONTROLLED NONLINEARITIES FOR STRUCTURAL DYNAMICS

Imre Gal[1]
Sebastiano Fichera[2], John E. Mottershead[3],
University of Liverpool, Brownlow Hill 765, L69 7ZX, Liverpool, United Kingdom

ABSTRACT

Accurate prediction of the in-flight shape of aircraft wings is essential for achieving optimal aerodynamic performance and structural efficiency. As modern aircraft wings become increasingly slender and flexible, their structural response is more strongly influenced by local stiffness variations, uncertainties, and nonlinear effects. These characteristics can lead to discrepancies between numerical predictions and experimentally observed behaviour, particularly when relying on idealised or linear structural models. Identifying and localising such effects is therefore critical, either to inform potential structural modifications or to provide guidance for future wing designs.

Traditionally, the in-flight shape is only known following the first flight of the aircraft, at which point the design has already matured and any further changes to the structure would be costly and difficult to introduce. The ground vibration test is the first moment in the design process where engineers collect the experimental datasets. Prior to which, only simulated data are available. These physical measurements are the first real information regarding the wing, and they are oftentimes differing from the numerical values. Traditionally, model updating techniques are then used to update the numerical models to better match the experimental measurements. However, by doing this, the target responses in case of the wing the target in-flight shape defined in the numerical models is lost.

In this work, a novel experimental rig has been developed with the purpose of representing the wing box of an aircraft wing in a discretised fashion, being able to reproduce the type of bending observed in real wings. The rig consists of three rigid elements, m_1, m_2, m_3, made from hollow aluminium bars, connected to each other through low friction ball bearing joints, j_1, j_2, j_3, and leaf spring assemblies. The joints allow rotational movement while the stiffness at the connections is provided through the leaf springs. A schematic of the rig can be seen on Figure 1. The length of the leaf springs can be adjusted by moving the connecting rigid elements, referred to as "bridge" and positioned alongside the springs, Figure 2. shows four configurations of the bridge locations, while Figure 3. shows the effect of these configurations on the structures frequency response function (FRF). It can be seen that, as the length of the springs is reduced, the stiffness of the structure increases, indicated by the shift of the first three natural frequencies to higher values.

---

[1] PhD candidate, Department Mechanical and Aerospace Engineering
[2] Senior Lecturer, Department of Aeronautics and Astronautics
[3] Emeritus Professor, Department Mechanical and Aerospace Engineering

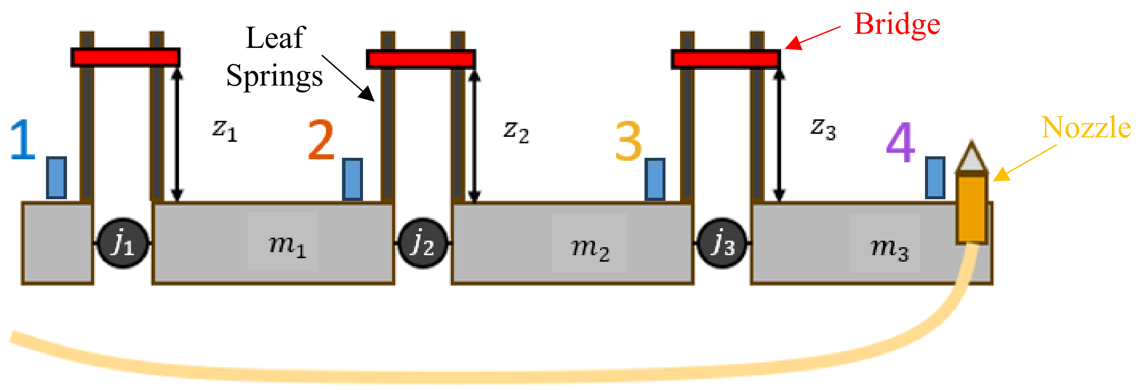

***Figure 1**. Schematic of experimental rig, blue squares are accelerometers with corresponding numbering in colour*

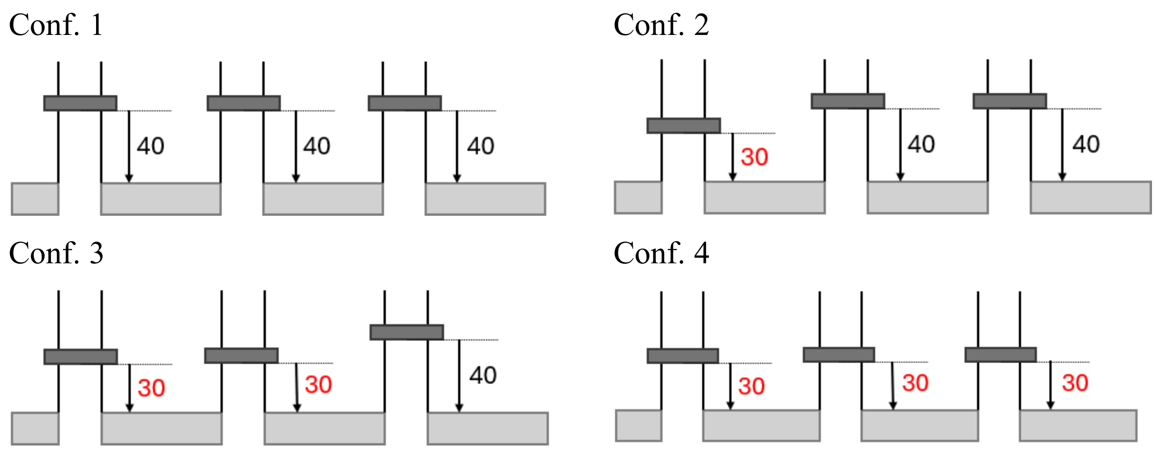

***Figure 2.** Four potential configurations. For the given cases Conf. 1 has the least stiffness while Conf.4 has the highest stiffness*

Aerodynamic loads can be simulated through a non-contact actuator formed by a compressed air-nozzle system placed at the tip of the structure. In its undeflected shape the structure corresponds to the jig shape of an aircraft wing, while when deflected it imitates the in-flight shape. Since no stingers or any form of mechanical attachments are used to achieve the in-flight shape, which could constrain the structure and influence its dynamic behaviour, operational modal testing becomes possible. All the conventional ground test campaign steps can be made on the jig-shape of the rig. In contrast to wing models normally used for wind tunnel and structural testing, users have the capability of easily modifying the local stiffness of the proposed rig at three locations, through adjusting the previously mentioned bridge locations, influencing the overall bending stiffness. Additionally, any form of user defined nonlinearity can be introduced into the structure through a brushless motor. Using a laser displacement sensor, either displacement or velocity measurements can be obtained at selected locations along the structure. These measurements are used as feedback to define stiffness- or damping-type nonlinearities, respectively. Through a hardware-in-the-loop (HIL) framework, users prescribe the desired stiffness or damping characteristics, which, in combination with the measured response, are used to command a brushless motor to apply a corresponding rotation at the joint, thereby introducing the targeted nonlinear behaviour. With this approach, a rotation applied in opposition to the structural motion results in a hardening nonlinearity, whereas a rotation applied in phase with the structural motion produces a softening nonlinearity, which is more challenging to realise experimentally. A simple schematic of the concept is shown in

Figure 4.

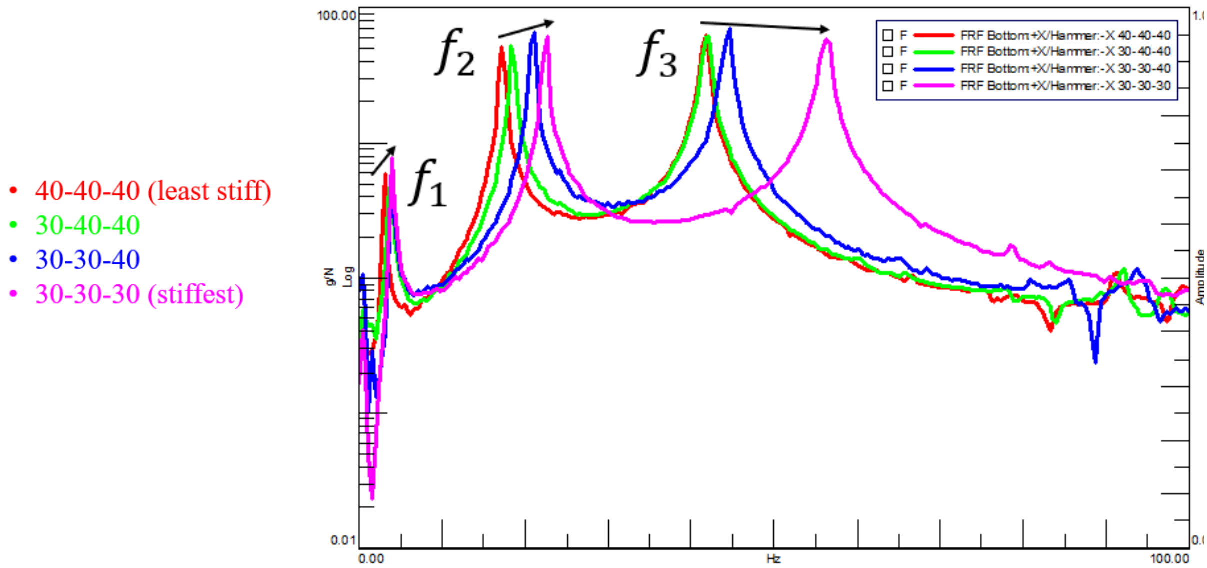

__Figure 3__. FRF plots corresponding to the four configurations. First three natural frequencies shown alongside with an arrow indicating their shift in their frequency values, caused by structural stiffness increase

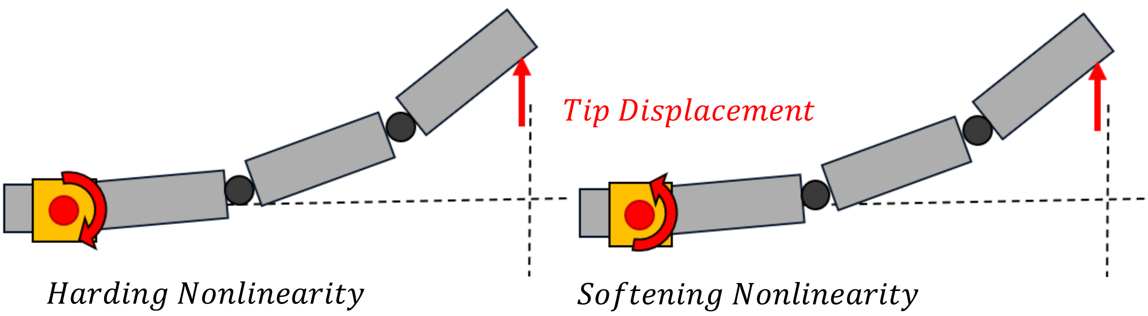

Figure 4. *Schematic of the use of brushless motor to introduce nonlinearities, on the left a hardening nonlinearity opposing structural rotation, on the right a softening nonlinearity in-phase with structural rotation*

The possibility of deliberately introducing uncertainties into the structure and being able to easily conduct tests on both the jig and in-flight shape makes the rig an ideal benchmark structure for uncertainty quantification exercises, nonlinearity localisation and identification techniques, and for development of shape predictive strategies. A photo of the rig is visible on Figure 5. (a), Figure 5. (b) shows the brushless motor and its connection to the first joint used to introduce nonlinearities.

In a previous work, sensitivity-based model updating principles were used to calibrate the physical structural stiffness, so it better matches the numerical model outputs. This process, referred to as *structure updating* sees the model updating workflow flipped. In this follow up work, the structure is expanded with a nonlinearity, and its localisation and identification will be examined using various of strategies.

First a nonparametric approach based on linear frequency response functions and nonlinear orthogonal projections [1,2] has been used on the Simulink model of the rig. In this method the nonlinear system is viewed as a linear system with a nonlinear feedback loop, in the frequency domain expressed as,

$$\mathbf{X}(\omega) = \mathbf{H}(\omega)(\mathbf{F}(\omega) - \mathbf{f}_{nl}(\omega)) \quad 1.$$

where, $\mathbf{X}(\omega)$ is the matrix of total responses, $\mathbf{H}(\omega)$ is the linear transfer function matrix, $\mathbf{F}(\omega)$ is the vector of linear external forces, and $\mathbf{f}_{nl}(\omega)$ is the vector of nonlinear restoring forces. Since, $\mathbf{F}(\omega)$ is known the linear and nonlinear part of the of the responses can be separated through the QR decomposition,

$$\mathbf{QR} = [\mathbf{F}^{\mathbf{T}}\ \mathbf{X}^{\mathbf{T}}] \quad 2.$$

This gives the vector of uncorrelated nonlinear responses, $\boldsymbol{X}_{unl}$.

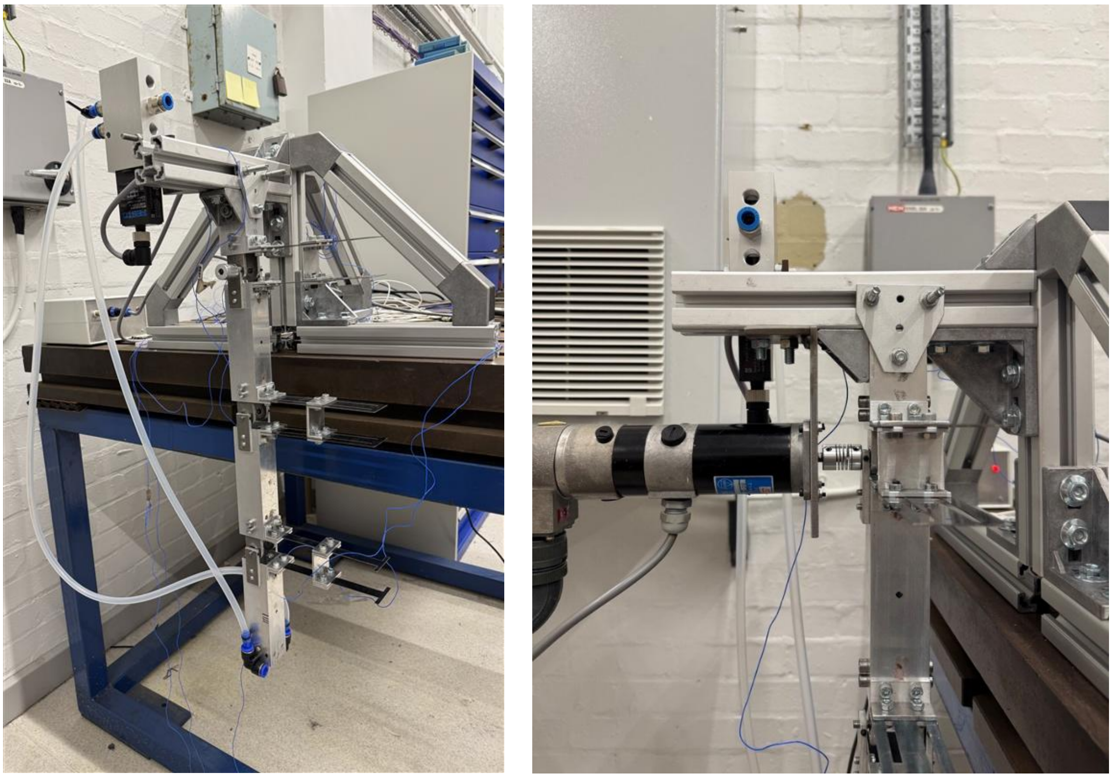

Figure 5. *(a) Photo of the experimental set-up, (b) Photo of the brushless motor and connection to the first joint*

Three cases have been examined, in the first two cases a cubic stiffness has been applied on the rotational degree of freedom of joint 1 and joint 2 respectively, j_1 and j_2 on Figure 1. and for the third case a quadratic damping has been applied on the rotational degree of freedom of joint 3, j_3. The nonlinearity location has been identified by comparing the columns of the linear frequency response function to the uncorrelated nonlinear response through the frequency response assurance criteria (FRAC). A FRAC value of one through the tested frequency range indicates the location of the nonlinearity. Results of the simulated cases can be seen of Figure 6, in all cases the nonlinearity location was successfully identified.

The proceedings will contain the FRAC based nonlinearity localisation results using experimental data, alongside with two additional methods capable of localisation of multiple nonlinearities. The first one is based on the previously mentioned method, but instead of the FRAC the inverse calculation of the restoring forces Equation. 3,4 and their corresponding values based on the accelerometer locations will be used for the localisation.

$$\mathbf{X}_{nl} = \mathbf{X}(\omega) - \mathbf{X}_{lin}(\omega) = -\mathbf{H}(\omega)\boldsymbol{f}_{nl}(\omega) \quad 3.$$

$$\mathbf{f}_{nl}(\omega) = -\mathbf{H}^{-1}(\omega)\mathbf{X}_{nl}(\omega) \quad 4.$$

The second method will be a parametric localisation and identification of nonlinearities based on describing function inversion. The latter strategy utilises the sum of the nonlinearity indices, Equation 5. as the localisation metric, while identification can be done through comparison of the calculated describing functions footprints to known nonlinear describing function footprints.

$$\boldsymbol{NLI}_p = \boldsymbol{\delta}_{ip} - \mathbf{H}_{p1}^{-1}\mathbf{H}_{1i}^{nl} - \mathbf{H}_{p1}^{-1}\mathbf{H}_{1i}^{nl} - \cdots - \mathbf{H}_{pn}^{-1}\mathbf{H}_{ni}^{nl} \quad 5.$$

where NLI is the nonlinearity index, δ_{ip} is Kronecker delta, subscripts p, i are the driving point location and response channel id respectively. This method also requires at least the measurement of a column of the nonlinear frequency response function, $\mathbf{H}^{nl}(\omega)$. The parametric identification is achieved through calculating the restoring forces by describing function inversion and data fitting.

The overall goal of the projects is to replicate the ground testing campaign of a wing and fully utilise the data available at this stage to provide suggestions of potential areas having uncertainties which were not captured by the simulations. Combining the nonlinearity identification methods with the structure updating procedure in order to improve the in-flight shape prior to the first deflection. The experimental rig allows to test hypotheses and see the proposed methods effectiveness

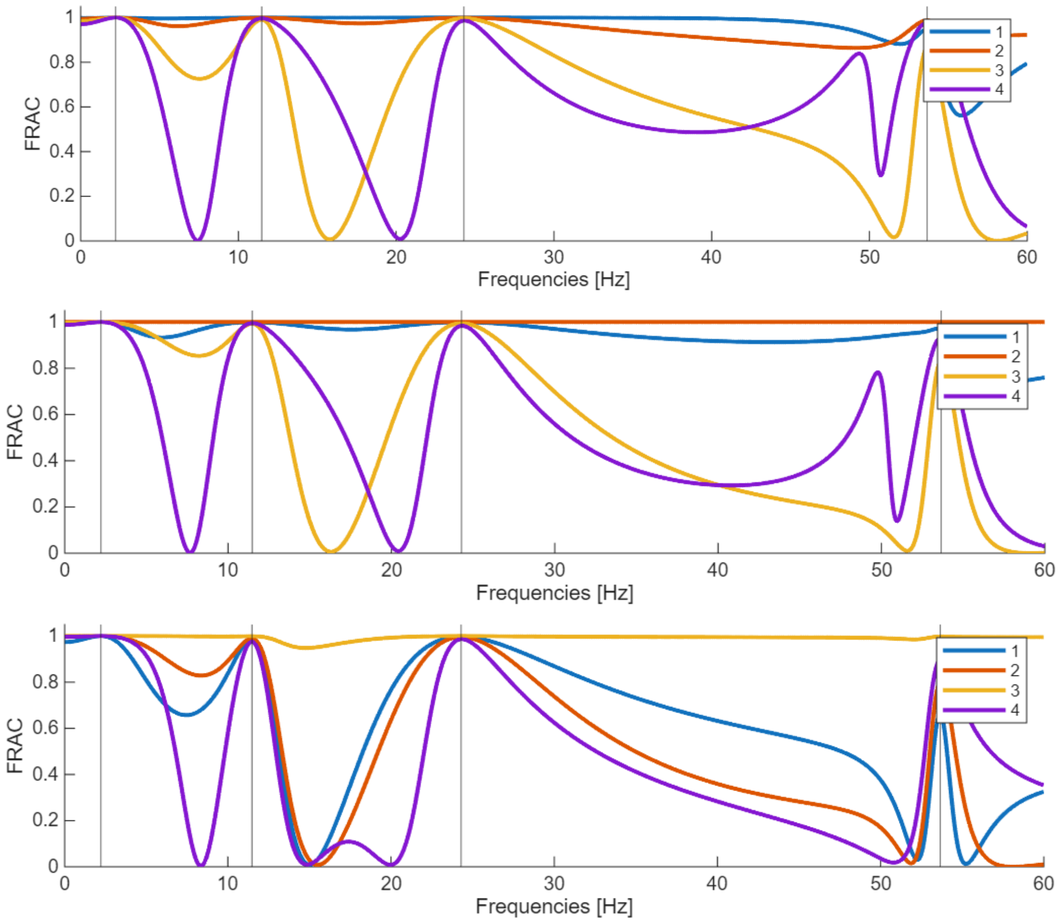

***Figure 6** Results of the nonlinearity localisation, Top FRAC of case 1, Middle FRAC of case 2, Bottom FRAC of case 3*

Acknowledgement

This work was carried out as part of a collaborative project between the University of Liverpool and Airbus. The authors would like to thank the Airbus correspondents Francesco Gambioli, Edoardo Menga, and Irma Isnardi for their valuable support and contributions.

References

[1] G. Kosova, E. Di Lorenzo, B. Peeters, G. Kerschen, Locating structural nonlinearities using linear frequency response functions and nonlinear orthogonal projections, Mech. Syst. Signal Process. 202 (2023) 110585
[2] Murali M. Kolluri, Randall J. Allemang, Allyn W. Phillips, Non-parametric detection and localization of structural nonlinearities using orthogonal projections, Mech. Syst. Signal Process. 123 (2019) 455–465,
[3] M. Aykan, H. Nevzat Özgüven, Parametric identification of nonlinearity in structural systems using describing function inversion, Mech. Syst. Signal Process. 40 (2013) 356–376,